Exploring the Space of Embedded Minimal Surfaces of Finite Total Curvature

Martin Traizet

CONTENTS

2000 AMS Subject Classification: Primary 53A10

Keywords: Minimal surface, balanced configuration, opening nodes

We investigate, both numerically and mathematically, several questions about embedded minimal surfaces of finite total curvature in Euclidean space. We also describe how a theoretical construction can be implemented numerically to produce pictures of such surfaces.

1. INTRODUCTION

This paper investigates the space of complete embedded minimal surfaces of finite total curvature (FTC) in Euclidean space. For a long time, the only known examples were the plane and the catenoid. In 1982, C. Costa discovered a genus-one example with three ends [Costa 84]. D. Hoffman and W. Meeks proved that the Costa surface is embedded, and they constructed, for each genus ≥ 1, a one-parameter family of embedded FTC minimal surfaces with three ends [Hoffman and Meeks 90]. Since then, several general methods to construct examples have been proposed [Weber and Wolf 02, Kapouleas 97].

In [Traizet 02], the author developed a construction that does not rely on symmetries, as do the previous ones. The input data for this construction is a finite collection of points in the complex plane (the *configuration*) satisfying a set of algebraic equations (the *balancing condition*). The output is a family of embedded FTC minimal surfaces, whose geometry can be described explicitly from the configuration. Roughly speaking, the surface is composed of planes with small catenoidal necks between them, and the configuration gives the position of the necks, as shown in Figure 1.

There are two aspects of this construction that can be explored numerically. The first is the search for balanced configurations. Most of the interesting examples I have found were discovered numerically. Some of them can be fully understood mathematically. They provide numerical or mathematical answers to several interesting questions about embedded FTC minimal surfaces.

1058-6458/2008 $ 0.50 per page
Experimental Mathematics **17**:2, page 205

FIGURE 1. A configuration of type 3, 4, 1 and a genus-5 embedded minimal surface in the corresponding family. The stars, the circles, and the dot represent the points at levels 1, 2, and 3, respectively. The neck sizes are $c_1 = \frac{7}{4}$, $c_2 = 1$, and $c_3 \approx 2.34$.

The other aspect is pictures. How can we actually compute these minimal surfaces? Theoretically, they are constructed using the Weierstrass representation. The Riemann surface is defined by opening nodes, an explicit algebraic construction. Then three holomorphic 1-forms ϕ_1, ϕ_2, ϕ_3 (the Weierstrass data) are defined abstractly by prescribing periods. The question is how these holomorphic 1-forms can be computed numerically. We provide a constructive answer to this problem when all parts of the noded Riemann surface have genus zero, and we explain how this can be used to implement the construction in [Traizet 02].

See http://www.lmpt.univ-tours.fr/~traizet/minimal.html for 3D versions of the images in this paper, which can be freely rotated using the mouse. The webpage http://www.lmpt.univ-tours.fr/~traizet/maple.html contains Maple 9 worksheets for the computations described in this paper.

2. BALANCED CONFIGURATIONS

A *configuration* is a collection of points $\{p_{k,i} : 1 \leq k \leq M,\ 1 \leq i \leq N_k\}$ in the complex plane, together with some positive real numbers $c_1, \dots, c_M$. These points are organized into layers: the points $p_{k,1}, \dots, p_{k,N_k}$ form the kth layer. There are M layers, and N_k points in the kth layer. We also say that the points $p_{k,1}, \dots, p_{k,N_k}$ are the points at level k. The total number of points is $N = N_1 + \cdots + N_M$. The numbers $c_1, \dots, c_M$ are called the *neck sizes*. The type of the configuration is the sequence $N_1, \dots, N_M$.

Given a configuration that is *balanced* and *nondegenerate* (we will explain these terms shortly), the output of [Traizet 02, Theorem 1] is a one-parameter family of FTC minimal surfaces $\{\mathcal{M}_s\}_{0<s<\varepsilon}$, for ε sufficiently small. These surfaces have genus $N - M$ and have $M + 1$ embedded ends, asymptotic to half-catenoids or planes. They can be described geometrically as $M + 1$ horizontal planes with small catenoidal necks between them; see Figure 2.

There are M layers of necks and N_k necks in the kth layer, whose positions are given by the points $p_{k,1}, \dots, p_{k,N_k}$. The necks in the kth layer have waist radius $\sim sc_k$. This geometric description holds only asymptotically as $s \to 0$.

The planes are perturbed to have logarithmic growth at infinity; the surface has $M + 1$ catenoid type ends, whose logarithmic growth is as follows: Let $Q_k = N_{k-1}c_{k-1} - N_k c_k$ (with the convention $N_0 = N_{M+1} = 0$). Then the logarithmic growth of the kth end is precisely sQ_k for $k = 1, \dots, M - 1$, and is asymptotically sQ_k for $k = M, M+1$ as $s \to 0$. (When the logarithmic growth is zero, the end is asymptotic to a plane.) The theorem also guarantees that if $Q_1 \leq \cdots \leq Q_{M-1} < Q_M < Q_{M+1}$, the surfaces $\mathcal{M}_s$ are embedded (for s sufficiently small). When this condition is satisfied, we say that the configuration is *embedded* (a rather clumsy but convenient terminology).

Let me now explain the balancing condition. Let

$$F_{k,i} = \sum_{\substack{j=1 \\ j \neq i}}^{N_k} \frac{2c_k^2}{p_{k,i} - p_{k,j}} - \sum_{j=1}^{N_{k-1}} \frac{c_k c_{k-1}}{p_{k,i} - p_{k-1,j}} - \sum_{j=1}^{N_{k+1}} \frac{c_k c_{k+1}}{p_{k,i} - p_{k+1,j}},$$

with the convention that $N_0 = N_{M+1} = 0$. Because of the analogy with 2-dimensional electrostatic forces, we

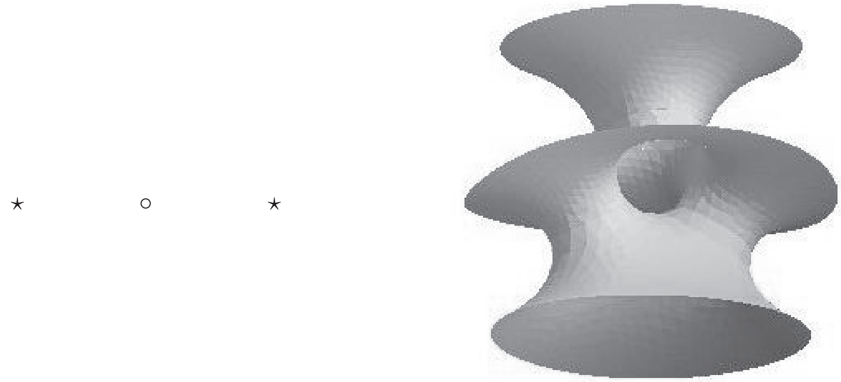

FIGURE 2. A genus-one Costa–Hoffman–Meeks surface, as computed from the configuration on the left.

call $F_{k,i}$ the *force* on $p_{k,i}$. The point $p_{k,i}$ interacts with all other points in the same layer and with the points in the layers directly below and above it. We require that the points in each layer be distinct and also that they be distinct from the points in the layers directly below and above, so that $F_{k,i}$ is defined. (We say that the configuration is *nonsingular*.)

The configuration is *balanced* if all forces are zero:

$$\forall k\ \forall i, \quad F_{k,i} = 0.$$

These are N algebraic equations. They are not independent because one has $\sum_{k,i} F_{k,i} = 0$. Moreover, a computation shows that

$$\sum_{k,i} p_{k,i} F_{k,i} = \sum_{k=1}^{M} n_k(n_k - 1)c_k^2 - \sum_{k=1}^{M-1} n_k n_{k+1} c_k c_{k+1}. \tag{2–1}$$

The right-hand side depends only on the neck sizes, and it must be equal to zero for balanced configurations to exist. When the neck sizes satisfy this condition, we are left with $N - 2$ equations to solve. The balancing condition is also invariant by translation and complex scaling of the points (transformations $z \mapsto az + b$). We may normalize the positions of two points, and are left with $N - 2$ parameters.

We call the configuration *nondegenerate* if the Jacobian matrix $\partial F_{k,i}/\partial p_{\ell,j}$ has complex rank $N - 2$. This is the maximum rank it may have.

2.1 Basic Example: Costa–Hoffman–Meeks

The simplest examples have $M = 2$ layers of necks, with $N_1 = n \geq 2$ and $N_2 = 1$. The neck sizes are $c_1 = 1$, $c_2 = n - 1$. The configuration has dihedral symmetry of order n and is given by $p_{1,i} = \omega^i$ and $p_{2,1} = 0$, where $\omega = \exp(2\pi \mathrm{i}/n)$. It is nondegenerate; for details, see [Traizet 02, Proposition 1].

The corresponding family of embedded FTC minimal surfaces is the Costa–Hoffman–Meeks family of genus $n-1$, or rather the extreme part of this family. (I have no proof of this claim, except by the classification in [Costa 89] in the genus-one case. All I really know is that the surfaces have the same symmetries and topology as the Costa–Hoffman–Meeks surfaces.)

These are also the only nondegenerate balanced configurations with two layers of necks; again see [Traizet 02, Proposition 1].

2.2 Dihedral Configurations

In this section we investigate the following question:

Question 2.1. What is the least genus for an embedded FTC minimal surface with $r \geq 2$ ends?

N. Kapouleas has proven the existence of embedded FTC minimal surfaces with any finite number of ends [Kapouleas 97]. His examples are constructed by desingularization of a finite set of coaxial catenoids and horizontal planes. However, the genera of his examples are very large by construction (in fact, it seems hard even to estimate the genus).

D. Hoffman and W. Meeks have conjectured that the answer to the above question is $r - 2$. M. Weber and M. Wolf have constructed, for each $r \geq 4$, an FTC minimal surface with genus $r - 2$ and r ends [Weber and Wolf 02]. However, they cannot mathematically prove that their examples are embedded, although numerically generated pictures seem to indicate that they are (at least for a few values of r).

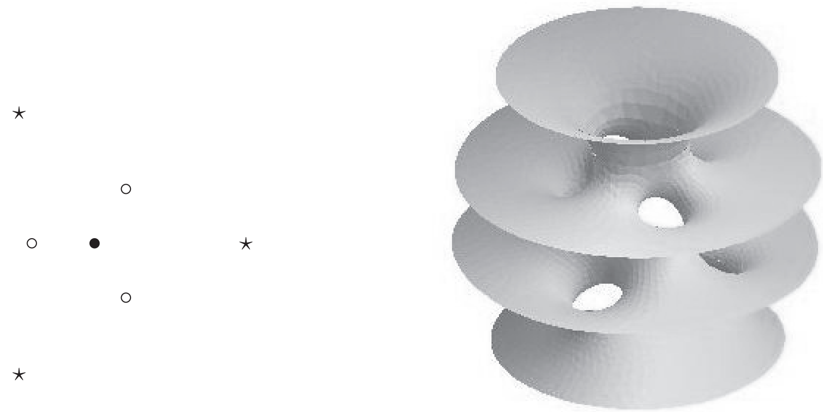

FIGURE 3. A configuration of type $3, 3, 1$ with dihedral symmetry and a genus-4 embedded minimal surface in the corresponding family. The neck sizes are $c_1 = 1.35$, $c_2 = 1$, and $c_3 = 1.595$.

Our result lies somewhere between these two: we can prove the existence of embedded FTC minimal surfaces with arbitrarily many ends, with an explicit formula for the genus, but the genus is not optimal.

The easiest way to compute balanced configurations with an arbitrary number of layers M is to retain the symmetries of the Costa–Hoffman–Meeks configuration and increase the number of layers (see Figure 3).

Let $M \geq 2$ be the number of layers. Take $N_1 = \cdots = N_{M-1} = n$ and $N_M = 1$, where $n \geq 2$ is some integer. We want the configuration to have dihedral symmetry of order n, so we set

$$p_{k,i} = a_k \omega^i, \quad 1 \leq k \leq M-1, \;\; p_{M,1} = 0,$$

where $\omega = \exp(2\pi \mathrm{i}/n)$ and a_k is such that $a_k^n \in \mathbb{R}^*$. Equation (2–1) gives

$$\sum_{k=1}^{M-1} n(n-1)c_k^2 - \sum_{k=1}^{M-2} n^2 c_k c_{k+1} = n c_{M-1} c_M. \qquad (2\text{–}2)$$

This determines c_M as a function of the parameters $c_1, \ldots, c_{M-1}$.

By symmetry, $F_{M,1} = 0$, and $p_{k,i}F_{k,i}$ is the same for all i. In fact, elementary computations give

$$p_{1,i}F_{1,i} = (n-1)c_1^2 - n c_1 c_2 \frac{a_1^n}{a_1^n - a_2^n}, \qquad (2\text{–}3)$$

and for $2 \leq k \leq M-2$,

$$p_{k,i}F_{k,i} = (n-1)c_k^2 - n c_{k-1} c_k \frac{a_k^n}{a_k^n - a_{k-1}^n} - n c_k c_{k+1} \frac{a_k^n}{a_k^n - a_{k+1}^n}. \qquad (2\text{–}4)$$

We can fix $a_1 = 1$, and then these equations determine recursively $a_2, \ldots, a_{M-1}$ as functions of $c_1, \ldots, c_{M-1}$. The equation $p_{M-1,i}F_{M-1,i} = 0$ is then automatically satisfied, since $\sum p_{k,i}F_{k,i} = 0$. Alternatively, we can choose the values of $a_1, \ldots, a_{M-1}$, and then the equations determine the values of $c_1, \ldots, c_{M-1}$.

For $M = 2$ we recover the Costa–Hoffman–Meeks configurations (see Section 2.1). For $M \geq 3$, these configurations yield minimal surfaces with $r = M + 1$ ends and genus $g = (n-1)(M-1)$. In particular, if $n = 2$, the genus is $g = r - 2$, the critical case for the Hoffman–Meeks conjecture. Unfortunately, it is not hard to check that when $M \geq 3$ and $n = 2$, the configuration is never embedded, whatever the choices of the neck sizes. I believe (this is pure speculation) that the surfaces we obtain in this case are in the same family as the examples constructed in [Weber and Wolf 02] but that these examples do not stay embedded all the way.

One question we have to answer is whether the above configurations are nondegenerate. It turns out that if $M \geq 3$, they are not always nondegenerate, but the following is true: for *generic* values of the parameters $c_1, \ldots, c_{M-1}$, the configuration is nondegenerate. Here generic means outside the zero set of a nonzero polynomial. Indeed, nondegeneracy can be written as a polynomial equation in $c_1, \ldots, c_{M-1}$.

To prove the statement, it suffices to prove that this polynomial is not identically zero, so it suffices to exhibit one set of values of the parameters such that the configuration is nondegenerate, for each n and M. We give the details of this computation in Section 4.1. It is clear that for generic values of $c_1, \ldots, c_{M-1}$, the configuration is nonsingular, which in this case means that all a_k are nonzero and $a_k \neq a_{k+1}$.

It remains to choose the neck sizes such that the configuration is embedded. Take $c_1 = \cdots = c_{M-1} = 1$. Equation (2–2) gives $c_M = n - M + 1$. Then $Q_1 = -n$, $Q_2 = \cdots = Q_{M-1} = 0$, $Q_M = M - 1$, and $Q_{M+1} = n - M + 1$. The condition $Q_{M+1} > Q_M$ gives $n > 2(M-1)$, so we can take $n = 2M - 1$. We obtain a family of embedded minimal surfaces with genus $2(M-1)^2$ and number of ends equal to $M+1$. This gives us the following theorem:

Theorem 2.2. *For each $r \geq 3$, there exists an embedded FTC minimal surface with r ends and genus $2(r-2)^2$.*

This estimate is by no mean optimal, since the genus grows quadratically with r, whereas the Hoffman–Meeks conjecture asks for linear growth. It is possible to improve this estimate, but not very much. In fact, it is possible to prove that in general, for a configuration with M layers, if the total number of necks is less than $M(M-1)/2$, the configuration cannot be embedded, whatever the repartition of the necks and the neck sizes. Hence one cannot construct minimal surfaces with r ends and genus less than $(r-1)(r-2)/2$ with this approach: quadratic growth of the genus cannot be avoided.

2.3 Asymmetric Configurations

In this section we investigate the following question:

Question 2.3. What is the least genus for an embedded FTC minimal surface with no symmetries?

By a symmetry, I mean an ambient isometry preserving the surface (other than the identity). In [Traizet 02], an embedded, asymmetric example of genus 45 with five ends was proven to exist, as well as examples of arbitrarily high genus.

A numerical search gives a large number of embedded asymmetric examples of much smaller genus. The smallest genus I have found so far is 6 (see Figure 4). Also, this numerical investigation has uncovered a genus-7 example that is simple enough that it can be proven mathematically to exist (see Figure 5).

In this section, we explain how one can compute configurations without the help of symmetries, a situation quite opposite to that of Section 2.2. A proof for the genus-7 example of Figure 5 is given in Section 4.2.

The only nondegenerate configurations with $M = 2$ layers are the Costa–Hoffman–Meeks configurations. The simplest next case is $M = 3$ with $N_3 = 1$, which already gives many interesting examples. Let me explain how I compute examples in this particular case. The method generalizes to an arbitrary number of layers and necks, but is especially successful in this case.

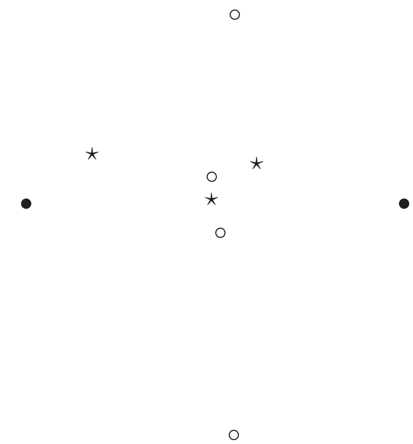

FIGURE 4. An asymmetric configuration of type 3, 4, 2 (embedded, genus 6). The neck sizes are $c_1 = \frac{7}{10}$, $c_2 = 1$, and $c_3 \approx 2.85$.

Note that the balancing condition is invariant by permutation of the points at each level, so we should not use $p_{k,i}$ as variables when computing configurations, for otherwise, each configuration will be duplicated $N_1!N_2!$ times, so the list of configurations will be huge, and in fact, the system will be impossible to solve. So the correct variables are the elementary symmetric functions of the points at each level.

Consider the polynomials

$$P_k(z) = \prod_{i=1}^{N_k}(z - p_{k,i}).$$

By translation, we may assume that $p_{3,1} = 0$, so $P_3 = z$. Let us write the forces in terms of P_1, P_2. We have

$$\frac{P_k'}{P_k}(z) = \sum_i \frac{1}{z - p_i} \qquad \text{if } P_k(z) \neq 0,$$

$$\frac{P_k''}{P_k'}(p_{k,i}) = \sum_{j \neq i} \frac{2}{p_{k,i} - p_{k,j}},$$

$$F_{k,i} = c_k^2 \frac{P_k''}{P_k'} - c_k c_{k-1} \frac{P_{k-1}'}{P_{k-1}} - c_k c_{k+1} \frac{P_{k+1}'}{P_{k+1}},$$

evaluated at $z = p_{k,i}$. From this we get that the configuration is balanced if the polynomial

$$c_1^2 z P_1'' P_2 + c_2^2 z P_2'' P_1 - c_1 c_2 z P_1' P_2' - c_2 c_3 P_1 P_2' \qquad (2\text{–}5)$$

vanishes at the points $p_{1,1}, \ldots, p_{1,N_1}$ and $p_{2,1}, \ldots, p_{2,N_2}$.

Since these are $N_1 + N_2$ distinct points and this polynomial has degree $\leq N_1 + N_2 - 1$, it is identically zero. Writing that all coefficients of this polynomial are zero gives a system of $N_1 + N_2$ quadratic equations in the coefficients of P_1, P_2. The leading coefficient of (2–5) is

$$N_1(N_1-1)c_1^2+N_2(N_2-1)c_2^2-N_1N_2c_1c_2-N_2c_2c_3, \quad (2\text{–}6)$$

so we recover equation (2–1). We are left with N_1+N_2-1 equations to solve. The unknowns are the $N_1 + N_2$ coefficients of P_1 and P_2.

This system has a special form that makes it relatively easy to solve. First of all, the balancing condition is invariant by complex scaling $z \mapsto az$, so we may normalize one coefficient of P_2 to be equal to 1. We may then use the first N_1 equations to express the coefficients of P_1 as functions of the coefficients of P_2, solving a *linear* system of N_1 equations. By substitution in the last $N_2 - 1$ equations, we obtain a system of algebraic equations in the $N_2 - 1$ remaining coefficients of P_2. This works fairly well if N_2 is small. If N_1 is small, we can exchange the roles of P_1 and P_2.

Once we have found a pair of polynomials P_1, P_2 satisfying (2–5), we recover a configuration by computing their zeros $p_{1,1}, \dots, p_{1,N_1}$ and $p_{2,1}, \dots, p_{2,N_2}$. We still must check that the configuration is *nonsingular*, in the sense that these points are distinct, so that the forces are defined. In fact, (2–5) always has the trivial solution $P_k = z^{N_k}$, which gives a useless configuration in which all points are equal to 0. But we can make sure a priori that any other solution is nonsingular as follows.

Note that the balancing condition does not make sense for a singular configuration, but equation (2–5) still does, and may be seen as a way to make sense of a balanced singular configuration. In fact, families of configurations typically become singular for some particular values of the neck sizes, although this can happen only for a finite number of values. To understand why, assume that z_0 is a zero of P_k with multiplicity $m_k \leq N_k$, for $k = 1, 2, 3$ (if $m_3 = 1$, then $z_0 = 0$). Assume that $m_1 + m_2 \geq 2$ or $m_2 + m_3 \geq 2$, so the configuration is singular. Also assume that $(m_1, m_2, m_3) \neq (N_1, N_2, N_3)$, since otherwise, $P_k = z^{N_k}$ for $k = 1, 2, 3$, and we have the trivial solution to (2–5).

Writing $P_k = \lambda_k(z-z_0)^{m_k} + o((z-z_0)^{m_k})$ and replacing in (2–5), we obtain the equation

$$m_1(m_1-1)c_1^2+m_2(m_2-1)c_2^2-m_1m_2c_1c_2-m_2m_3c_2c_3 = 0. \quad (2\text{–}7)$$

Eliminating c_3 from (2–6) and (2–7), we obtain a quadratic homogeneous equation in the unknowns c_1, c_2, whose coefficients depend on (m_1, m_2, m_3).

By inspection, we find that the coefficients of this equation are not all zero, so normalizing by $c_1 = 1$, there are at most two possible values for c_2. Since there is only a finite number of possible values for the triple (m_1, m_2, m_3), there is only a finite number of values of c_2 for which a singular configuration (besides the trivial solution $P_k = z^{N_k}$) can occur.

Figure 5 displays a configuration of type $5, 4, 1$. This configuration is almost singular, and it becomes singular when $c_2 = 1$. One can compute the configuration quite explicitly by hand when $c_2 = 1$, and conclude that it is asymmetric. The details of this computation are given in Section4.2. This proves the following theorem:

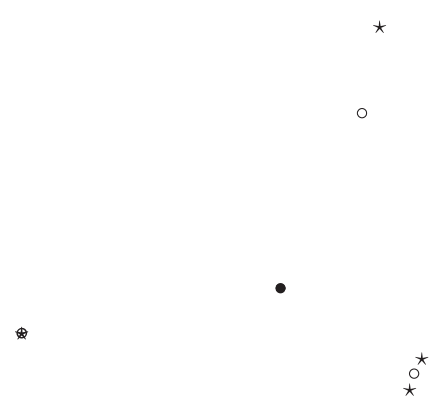

FIGURE 5. An asymmetric configuration of type $5, 4, 1$. The neck sizes are $c_1 = 1$, $c_2 = 1.01$, and $c_3 \approx 2.98$. There is a cluster of four points on the left and a cluster of three points on the right. This configuration is almost singular.

Theorem 2.4. *There exist embedded asymmetric FTC minimal surfaces of genus 7 with four ends.*

2.4 A Minimal Surface with a Planar End of Order 2

In this section we investigate the following question :

Question 2.5. Can an embedded FTC minimal surface have a planar end of order two?

We are talking here about the order of the extended Gauss map at the puncture corresponding to the end. This order is always at least 2 for a planar end. There are examples of periodic minimal surfaces with planar ends of order 2, such as the Riemann minimal examples. For the previously known examples of FTC minimal surfaces with planar ends, the order of the Gauss map at the end was always at least 3. But this was in fact forced by the symmetries of these surfaces. In this section we exhibit an example with a planar end of order 2.

We consider a configuration of type $5, 4, 1$. We may normalize $c_1 = 1$, and we choose $c_2 = \frac{5}{4}$. Equation (2–1) gives $c_3 = \frac{11}{4}$. The logarithmic growths of the ends are $Q_1 = -5$, $Q_2 = 0$, $Q_3 = \frac{9}{4}$, $Q_4 = \frac{11}{4}$, so the end at level 2 is planar. The configuration can be computed as in Section 2.3.

The question is, how can we determine the order of the Gauss map at the planar end? Theoretically, we have the following asymptotic for the Gauss map g_s of $\mathcal{M}_s$ in a neighborhood of the planar end (corresponding to $z = \infty$):

$$\lim_{s\to 0} -2(sg_s(z)^{-1}) = \sum_{i=1}^{N_1} \frac{c_1}{z - p_{1,i}} - \sum_{i=1}^{N_2} \frac{c_2}{z - p_{2,i}}.$$

The right-hand side can be expanded as

$$(N_1c_1 - N_2c_2)z^{-1} + \Big(c_1 \sum_{i=1}^{N_1} p_{1,i} - c_2 \sum_{i=1}^{N_2} p_{2,i}\Big) z^{-2} + o(z^{-2}).$$

The first term vanishes because the end is planar. The Gauss map has order 2 if the second term is not zero. This condition is easy to check (note that we do not need to compute the points $p_{k,i}$; the coefficients of the polynomials P_k are enough).

The configuration can be computed using the methods of Section 2.3. Unfortunately, I was not able to prove mathematically (meaning by hand) that this configuration is nondegenerate. (What I can prove is that the configuration is nondegenerate for generic values of the neck sizes, but here the neck sizes are fixed.)

The computation can easily be done using software like Maple or Mathematica, however. Moreover, the computation involves only rational numbers, and so it can be carried out using exact arithmetic. This gives a numerical proof that there exist embedded FTC minimal surfaces with a planar end of order 2. The details of this computation are given in Section 4.3.

3. PICTURES

The goal of this section is to explain how, given a balanced configuration, one can compute numerically the corresponding family of minimal surfaces. This is illustrated in Figure 6 in the case of the Costa–Hoffman–Meeks genus-1 family (recall that this family corresponds to a configuration of type $2, 1$; see Section 2.1).

The surface is decomposed into three pieces, one for each end. Each piece is parameterized by a *multicircular domain*, by which I mean the complex plane minus one or several circular disks. The point at infinity corresponds to an end of the surface. (In practice, we clip the ends, so each piece is parameterized by a big disk minus some small disks.)

If we identify the circle marked A with the circle marked A', the circle marked B with the circle marked B', and the circle marked C with the circle marked C', we obtain topologically a genus-1 surface with three ends.

To see why this defines a Riemann surface, we must specify how we identify the circles with one another. This is in fact an instance of a standard construction called *opening nodes*, which is fundamental to the construction in [Traizet 02], so let me explain this construction in greater detail.

Consider three copies of the complex plane, labeled $\mathbb{C}_1$, $\mathbb{C}_2$, $\mathbb{C}_3$. Take two distinct points $a^-_{1,1}$, $a^-_{1,2}$ in $\mathbb{C}_1$, three distinct points $a^+_{1,1}$, $a^+_{1,2}$, $a^-_{2,1}$ in $\mathbb{C}_2$, and one point $a^+_{2,1}$ in $\mathbb{C}_3$. Identify

$$a^-_{1,1} \sim a^+_{1,1}, \quad a^-_{1,2} \sim a^+_{1,2}, \quad \text{and} \quad a^-_{2,1} \sim a^+_{2,1}.$$

This defines a (singular) Riemann surface with three nodes (or double points). The planes $\mathbb{C}_1$, $\mathbb{C}_2$, $\mathbb{C}_3$ are called the parts of the noded Riemann surface.

To open the nodes, we consider three nonzero complex parameters $t_{1,1}$, $t_{1,2}$, and $t_{2,1}$. We remove the disk $D(a^-_{k,i}, |t_{k,i}|)$ in $\mathbb{C}_k$ and the disk $D(a^+_{k,i}, |t_{k,i}|$ in $\mathbb{C}_{k+1}$, for (k,i) equal to $(1,1)$, $(1,2)$, and $(2,1)$. We identify the point z in the annulus $|t_{k,i}| < |z - a^-_{k,i}| < 1$ in $\mathbb{C}_k$ with the point z' in the annulus $|t_{k,i}| < |z' - a^+_{k,i}| < 1$ in $\mathbb{C}_{k+1}$ such that $(z - a^-_{k,i})(z' - a^+_{k,i}) = t_{k,i}$, for (k,i) equal to $(1,1)$, $(1,2)$, and $(2,1)$. This defines a Riemann surface because the change of coordinates $z \mapsto z'$ is holomorphic.

Let me explain how this construction is related to Figure 6. Note that the circle with center $a^-_{1,1}$ in $\mathbb{C}_1$ and the circle with center $a^+_{1,1}$ in $\mathbb{C}_2$, both of radius $\sqrt{|t_{1,1}|}$, are identified: these are the circles labeled A and A' in Figure 6. A similar statement holds for the other pairs of circles. As $t_{k,i}$ goes to zero, the corresponding circles collapse into the node. In some sense, the Riemann surface converges to the noded Riemann surface. The argument of $t_{k,i}$ may be seen as a Dehn twist parameter.

The parameters in this construction are the six points $a^{\pm}_{k,i}$ and the three complex numbers $t_{k,i}$, for a total of nine complex parameters. We can, however, normalize the value of six parameters by translation and complex scaling in each plane.

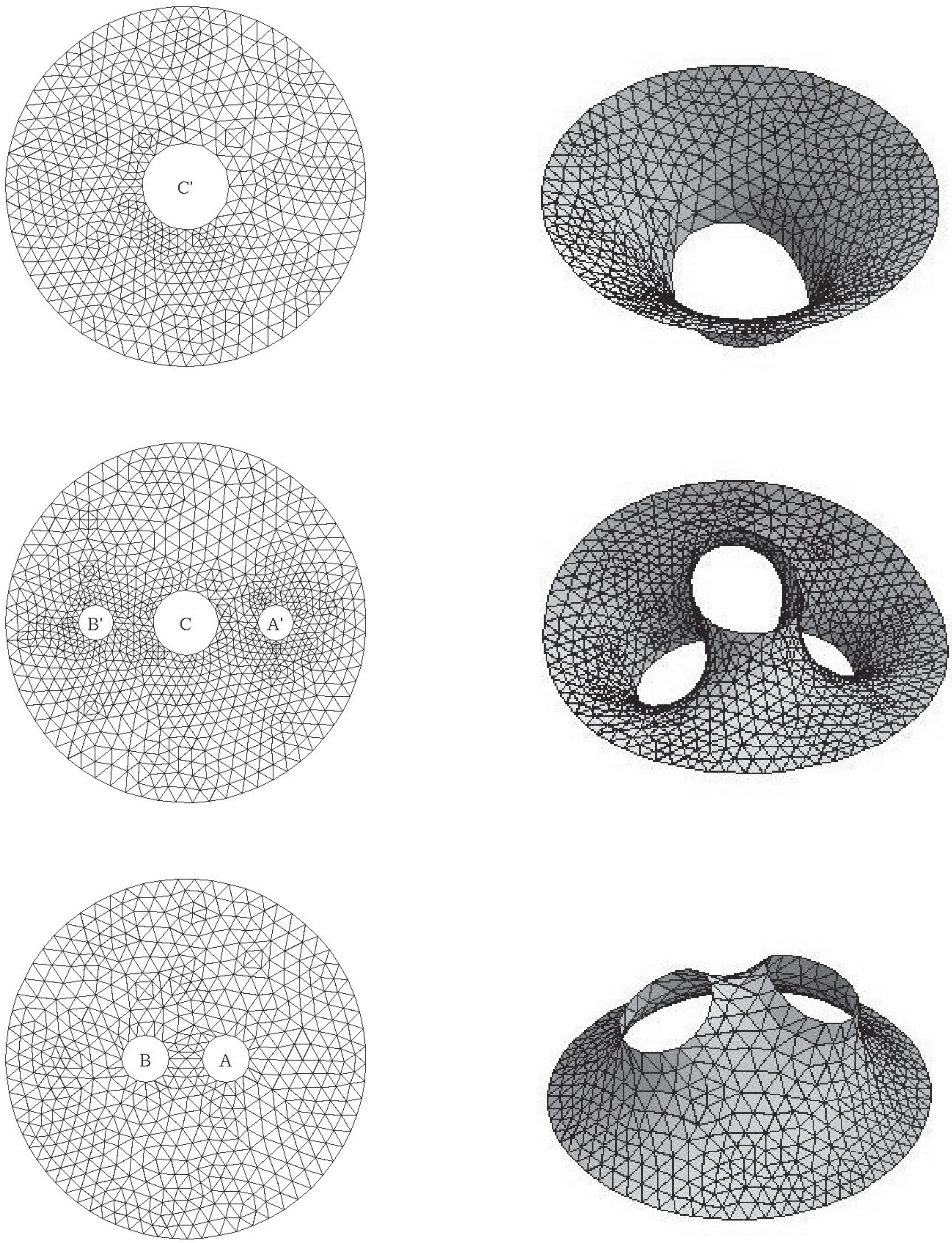

FIGURE 6. Triangulation of the three multicircular domains generated with MATLAB (left) and their image in space (right), in the case of the Costa–Hoffman–Meeks genus-1 surface. The three pieces on the right match perfectly, to give the whole surface.

Then we are left with three complex parameters, which is the dimension of the space of conformal structures on a torus with three punctures.

More generally, in the case of a configuration of type $N_1, \dots, N_M$, we consider $M+1$ copies of the complex plane, labeled $\mathbb{C}_1, \dots, C_{M+1}$. We take $N_k + N_{k-1}$ distinct points $a^-_{k,1}, \dots, a^-_{k,N_k}$ and $a^+_{k-1,1}, \dots, a^+_{k-1,N_{k-1}}$ in $\mathbb{C}_k$ (with the convention $N_0 = N_{M+1} = 0$). We identify $a^-_{k,i} \sim a^+_{k,i}$ for each possible pair (k, i), which defines a noded Riemann surface with $N = N_1 + \cdots + N_M$ nodes. We open the nodes as explained above, introducing one parameter $t_{k,i}$ per node.

The minimal surface is parameterized by the Weierstrass representation in the following form:

$$X(z) = \left(\operatorname{Re} \int_{z_0}^{z} \phi_1, \operatorname{Re} \int_{z_0}^{z} \phi_2, \operatorname{Re} \int_{z_0}^{z} \phi_3 \right),$$

where ϕ_1, ϕ_2, and ϕ_3 are three holomorphic 1-forms on our Riemann surface such that $\phi_1^2 + \phi_2^2 + \phi_3^2 = 0$ (the conformality equation). The *period problem* requires that $X(z)$ be well defined (independent of the integration path).

To find three holomorphic 1-forms satisfying the conformality equation and the period problem, we adopt the following strategy: We construct ϕ_1, ϕ_2, ϕ_3 by prescribing their periods around the necks. (These periods are imaginary, so part of the period problem is already solved by definition. Each imaginary part is a parameter.) Then we adjust the parameters to solve $\phi_1^2 + \phi_2^2 + \phi_3^2 = 0$ and the remaining part of the period problem.

This strategy was used in [Traizet 06] to construct triply periodic minimal surfaces. We follow that construction, with a few modifications due to the fact that our minimal surfaces have ends.

This is not the strategy used to construct the family of minimal surfaces in [Traizet 02], where we used the classical form of the Weierstrass representation (with the Gauss map). The construction in [Traizet 02] seems more difficult to implement.

The main question we have to answer to implement the construction in [Traizet 06] is, how can we compute these holomorphic 1-forms numerically? For each of them, we need some kind of formula in each multicircular domain. We answer this question in Section 3.1. Each 1-form is represented by some kind of series, whose coefficients are determined by solving a linear system.

At this point we have a family of Riemann surfaces and holomorphic 1-forms ϕ_1, ϕ_2, ϕ_3, depending on a number of parameters. We have a well-defined immersion on each multicircular domain, but there is no reason that the images should fit together. For instance, in Figure 6, the images of the circles A and A' differ by a translation, and so do the images of the circles B and B'. But there is no reason that these translations should be the same (as is the case in Figure 6). We need to adjust the parameters so that this is the case, which is the period problem.

We also have to adjust the parameters so that $\phi_1^2+\phi_2^2+\phi_3^2 = 0$. Let $\psi = \phi_1^2 + \phi_2^2 + \phi_3^2$. This is a meromorphic quadratic differential with at most double poles at the ends. The space of such differentials has finite complex dimension $3N - M - 1$. The question is, how do we compute numbers from a quadratic differential?

Following the construction in [Traizet 06], we simply compute periods of ψ/dz along suitable circles in each multicircular domain (where dz stands for the usual dz in each multicircular domain, so it is not globally defined on our Riemann surface) and check that we obtain $3N - M - 1$ independent equations. (Another possibility would be to divide ψ by a global 1-form, say ϕ_3, and compute periods. It is much simpler numerically to compute periods of ψ/dz.)

The total number of (real) equations we have to solve is $9N-5M-3$. This is a quite large number of equations: for example, for the asymmetric example of Figure 7, with $N = 10$ and $M = 3$, we have 72 equations to solve. How do we solve such a large nonlinear system?

Theoretically, in [Traizet 06] we solve these equations using the implicit function theorem. The proof of that theorem, which is based on the contraction mapping principle, gives a method to compute the solution numerically: Assume that we have a system of n equations in n variables, depending on some parameter s, which we write as $f_s(x) = 0$. Assume that when $s = 0$, we are given a solution x_0, and we know that $A = df_0(x_0)$ is invertible. Then for s small, we can solve $f_s(x) = 0$ by the following iteration scheme: Define the sequence $\{x^k\}_{k\in\mathbb{N}}$ inductively by $x^0 = x_0$ and

$$x^{k+1} = x^k - A^{-1} f_s(x^k). \qquad (3\text{–}1)$$

Then for s small, $\{x^k\}_{k\in\mathbb{N}}$ converges to a solution x of $f_s(x) = 0$.

We apply this scheme to solve our equations. Without entering into too much detail, we note that at the point x_0, the underlying Riemann surface is fully noded (all $t_{k,i}$ are zero: the necks collapse to double points), and the center of the circles are given by the points of the configuration. We can compute explicitly all equations at this point; see [Traizet 06] for more details.

The equations boil down to the balancing condition. Moreover, we can compute explicitly the Jacobian matrix

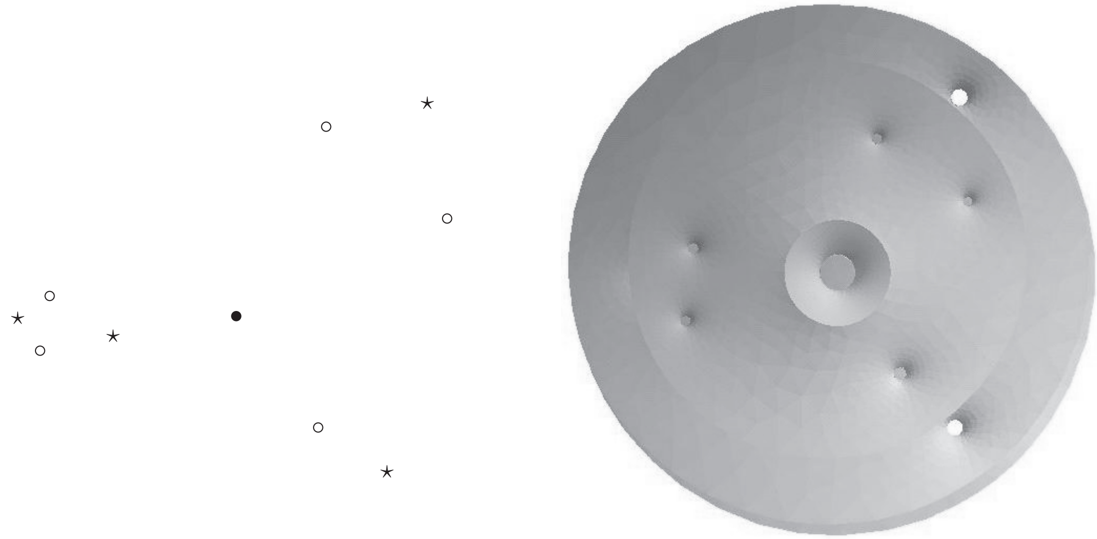

FIGURE 7. A genus-7 embedded asymmetric minimal surface (top view), computed from a configuration of type $4, 5, 1$. The neck sizes are $c_1 = \frac{3}{2}$, $c_2 = 1$, and $c_3 = \frac{17}{5}$.

A (derivatives of equations with respect to parameters) at the point x_0. Provided the configuration is nondegenerate, the Jacobian matrix is invertible. We then invert numerically the Jacobian and apply the iteration scheme (3–1). For small values of s it converges very quickly to a fixed point (several digits of precision are gained at each loop).

When we increase the value of s, the iteration no longer converges. Here is the idea to push the parameter s further: start from a previously computed solution x_s, increase s by a small amount, and apply again the above iteration scheme with $x^0 = x_s$ and A equal to the Jacobian at x_s.

The basic problem is that as soon as s is not zero, the nodes open (the $t_{k,i}$ are nonzero), so we cannot compute the Jacobian matrix explicitly.

However, we can compute a good approximation of the Jacobian by pretending that the Riemann surface is still noded. Because the radii remain quite small (even though the other parameters move considerably), this gives us an approximate Jacobian that we can use instead of A.

Finally, to plot the surface, we need to integrate ϕ_1, ϕ_2, ϕ_3. Because these 1-forms are represented as series, their integrals are readily computed: no numerical integration is required.

The rest of this section is organized as follows: in Section 3.1, we explain how we compute numerically a holomorphic 1-form defined by prescribing periods in the case of opening nodes. In Section 3.2, we give more details about the construction of the family of minimal surfaces.

3.1 Opening Nodes: A Model Case

In this section we explain how to compute holomorphic 1-forms on Riemann surfaces defined by opening nodes. For simplicity of notation, we first consider the case that the noded Riemann surface has only one part. Then we explain how one can generalize the construction to other cases.

Consider $2N$ distinct points $a_1^-, \dots, a_N^-, a_1^+, \dots, a_N^+$ in the complex plane. We assume for convenience that the disks of radius one centered at these points are disjoint. Identify for each $i = 1, \dots, N$ the point a_i^- with the point a_i^+. This defines a noded Riemann surface Σ_0 with N nodes, which we call $a_1, \dots, a_N$.

To open the nodes, consider N complex numbers $t_1, \dots, t_N$ such that $0 < |t_i| < 1$. Remove the $2N$ disks $D(a_i^\pm, |t_i|)$. Identify the annulus $|t_i| < |z - a_i^-| < 1$ with the annulus $|t_i| < |z' - a_i^+| < 1$ under the rule $(z - a_i^-)(z' - a_i^+) = t_i$. This defines an open Riemann surface Σ_t, where $t = (t_1, \dots, t_N)$. We compactify Σ_t by adding the point at infinity, and we still denote by Σ_t the compactification. The genus of Σ_t is N.

It is well known that the space of holomorphic 1-forms on Σ_t has complex dimension N, and that a holomorphic 1-form is uniquely defined by prescribing its periods on the circles around the points $a_1^+, \dots, a_N^+$. Let ω be the holomorphic 1-form on Σ_t defined by prescribing

$$\int_{C(a_i^+,1)} \omega = 2\pi \mathrm{i} c_i, \quad i = 1, \dots, N,$$

where $c_1, \dots, c_N$ are given complex numbers. How can we actually compute ω?

We are aiming for a formula of the form

$$\omega = \sum_{\pm} \sum_{i=1}^{N} \sum_{n=1}^{\infty} \frac{A_{i,n}^{\pm}}{(z - a_i^{\pm})^n} dz, \tag{3–2}$$

where the complex numbers $A_{i,n}^{\pm}$ are such that $A_{i,n}^{\pm} t_i^{-n}$ is bounded, so that the series converges on the domain $|z - a_i^{\pm}| > |t_i|$. (In the above formula, the sum over $\pm$ means that we add two terms, one for $+$ and one for $-$.) It is not hard to see that ω admits such a representation, using a Laurent series in the annuli $|t_i| < |z - a_i^{\pm}| < 1$ and the fact that a holomorphic 1-form on the Riemann sphere $\mathbb{C} \cup \{\infty\}$ must be identically zero.

The residues $A_{i,1}^{\pm}$ are determined by the prescribed periods: since the circle $C(a_i^+, 1)$ is homologous in Σ_t to the circle $C(a_i^-, 1)$ with the opposite orientation, we must have

$$A_{i,1}^{\pm} = \pm c_i.$$

(Note that this implies that the sum of all $A_{i,1}^{\pm}$ is zero, so ω is holomorphic at infinity.)

We want ω to be well defined on Σ_t, namely invariant under the identification rule used to define Σ_t. This should uniquely determine all coefficients $A_{i,n}^{\pm}$. Let

$$\varphi_i(z) = a_i^- + \frac{t_i}{z - a_i^+},$$

so φ_i maps the annulus $|t_i| < |z - a_i^+| < 1$ to the annulus $|t_i| < |z - a_i^-| < 1$, and Σ_t is defined by identifying z with $\varphi_i(z)$. The fact that ω is well defined on Σ_t is equivalent to $\varphi_i^* \omega = \omega$ on the annulus $|t_i| < |(z - a_i^+)| < 1$, for all $i = 1, \dots, N$. This is equivalent to

$$\forall m \in \mathbb{Z}, \quad \int_{C(a_i^+,1)} (z - a_i^+)^m \varphi_i^* \omega = \int_{C(a_i^+,1)} (z - a_i^+)^m \omega. \tag{3–3}$$

By a change of variable,

$$\int_{C(a_i^+,1)} (z - a_i^+)^m \varphi_i^* \omega = -\int_{C(a_i^-,1)} \left(\frac{t_i}{z - a_i^-} \right)^m \omega.$$

So (3–3) may be rewritten as

$$\forall m \geq 1, \quad A_{i,m+1}^{\pm} = -\frac{t_i^m}{2\pi \mathrm{i}} \int_{C(a_i^{\mp},1)} \frac{\omega}{(z - a_i^{\mp})^m}. \tag{3–4}$$

(Notation: the sign $\mp$ on the right side is opposite to the sign $\pm$ on the left side.) This is an infinite-dimensional linear system in the unknowns $A_{i,n}^{\pm}$, $n \geq 2$.

Let us introduce the following notation:

$$\omega_0 = \sum_{\pm} \sum_{i=1}^{N} \frac{\pm c_i}{z - a_i^{\pm}} dz,$$

$$A = (A_{i,n}^{\pm} \ : \ i \leq N, \ n \geq 2),$$

$$\alpha(A) = \sum_{\pm} \sum_{i=1}^{N} \sum_{n=2}^{\infty} \frac{A_{i,n}^{\pm}}{(z - a_i^{\pm})^n} dz,$$

$$F_{i,m}^{\pm}(\alpha) = -\frac{t_i^{m-1}}{2\pi \mathrm{i}} \int_{C(a_i^{\mp},1)} \frac{\alpha}{(z - a_i^{\mp})^{m-1}},$$

$$F(\alpha) = (F_{i,m}^{\pm}(\alpha) : i \leq N, \ m \geq 2).$$

Then (3–4) may be rewritten as $A = F(\omega_0 + \alpha(A))$.

We solve this fixed-point problem using the standard iteration scheme: define the sequence $\{A_k\}_{k \in \mathbb{N}}$ by induction, setting $A_0 = 0$ and $A_{k+1} = F(\omega_0 + \alpha(A_k))$. To see that $\{A_k\}_{k \in \mathbb{N}}$ converges to a fixed point, we introduce the following Banach norms:

$$\|A\| = \sum_{\pm} \sum_{i=1}^{N} \sum_{n=2}^{\infty} |A_{i,n}^{\pm}|,$$

$$\|\alpha\|_{\infty} = \sum_{\pm} \sum_{i=1}^{N} \sup_{z \in C(a_i^{\pm},1)} |\alpha(z)|.$$

Then straightforward estimates give

$$\|\alpha(A)\|_{\infty} \leq \|A\|,$$

$$\|F(\alpha)\| \leq \Big(\sum_{i=1}^{2N} \frac{|t_i|}{1 - |t_i|} \Big) \|\alpha\|_{\infty}.$$

Hence $\|F(\omega_0)\| < \infty$, and provided that all t_i are small enough, $A \mapsto F(\alpha(A))$ is a contracting linear operator. It follows, by the standard fixed-point theorem, that the sequence $\{A_k\}_k$ converges to a solution A of $A = F(\omega_0 + \alpha(A))$.

Let $\omega = \omega_0 + \alpha(A)$. From (3–4), we have the estimate

$$|A_{i,m}^{\pm}| \leq |t_i|^{m-1} \|\omega\|_{\infty}. \tag{3–5}$$

Hence each series $\sum_n A_{i,n}^{\pm}(z - a_i^{\pm})^{-n}$ converges for $|z - a_i^{\pm}| > |t_i|$, so ω is the desired 1-form.

What we have achieved is a constructive proof of the existence and uniqueness of ω on Σ_t, provided that all t_i are small enough. The above method generalizes easily to the case of *meromorphic* differentials with prescribed principal part at the poles, provided that the poles are outside the disks $D(a_i^{\pm}, 1)$: simply add the principal parts to ω_0.

The method also generalizes to the case of *several* Riemann spheres connected by nodes (see Section 3.2); the notation is just a bit more cumbersome. On the other hand, it is essential to the above argument that all the parts of the noded Riemann surface have genus zero so that we can represent ω as a series.

There are several reasons why a constructive proof is interesting. First of all, this allows us to compute ω numerically, which is our interest in this paper. The estimate (3–5) says that the coefficients $A_{i,n}^{\pm}$ decay rapidly with n, provided that all t_i remain small. So it is legitimate to truncate the series to some finite order. Typically for the examples we will consider, $|t_i|$ is of order 0.01, and we truncate the series to the order $n = 10$.

The method is also interesting from the theoretical point of view because it generalizes to the case of *infinitely many* Riemann spheres connected by nodes. In this case, by opening the nodes we obtain noncompact Riemann surfaces of infinite genus. The standard "abstract algebraic geometry" machinery does not seem to apply to this setup. It might be useful to construct, for instance, aperiodic minimal surfaces of infinite topology.

The integral in (3–4) can be explicitly computed using the following formula:

$$\mathrm{Res}_b \frac{1}{(z-a)^n (z-b)^m} = \binom{n+m-2}{m-1} \frac{(-1)^{m-1}}{(b-a)^{n+m-1}}.$$

3.2 Computing the Family of Minimal Surfaces

In this section, we give more details on how we compute numerically the family of minimal surfaces corresponding to a given configuration. As was already stated, we follow very closely the construction in [Traizet 06], with a few modifications due to the fact that our surfaces have catenoidal ends. In particular, the notation and normalizations are as in that paper. Giving all the details of the construction would essentially amount to a proof of the main theorem in [Traizet 02], which is not our purpose here, so we will be quite allusive.

Given a configuration of type $N_1, \ldots, N_M$, a family of Riemann surfaces is constructed by opening nodes, as explained at the beginning of Section 3. The parameters in this construction are the points $a_{k,i}^{\pm}$ and the complex numbers $t_{k,i}$ used to open the nodes. We compactify the Riemann surface by adding the points at infinity $\infty_1, \ldots, \infty_{M+1}$. Let Σ_t be the resulting compact Riemann surface.

Next we define three meromorphic 1-forms ϕ_1, ϕ_2, ϕ_3 on Σ_t, with poles at $\infty_1, \ldots, \infty_{M+1}$, by prescribing periods on the circles $C(a_{k,i}^{+}, 1)$ as explained in Section 3.1. The principal parts at the poles are forced by the fact that we want horizontal catenoidal (or planar) ends: ϕ_1 and ϕ_2 need double poles, with no residue, and ϕ_3 needs a simple pole (or no pole in the planar case).

As explained in Section 3.1, we represent ϕ_ν as

$$\phi_{\nu,k} = \lambda_{\nu,k} dz + \sum_{i=1}^{N_k} \sum_{n=1}^{\infty} \frac{A_{\nu,k,i,n}^{-}}{(z - a_{k,i}^{-})^n} dz + \sum_{i=1}^{N_{k-1}} \sum_{n=1}^{\infty} \frac{A_{\nu,k-1,i,n}^{+}}{(z - a_{k-1,i}^{+})^n} dz. \tag{3–6}$$

Here $\phi_{\nu,k}$ denotes ϕ_ν in $\mathbb{C}_k$. The first term takes care of the double pole at ∞_k. We require that

$$\lambda_{1,k} = 1, \quad \lambda_{2,k} = (-1)^{k+1}\mathrm{i}, \quad \lambda_{3,k} = 0.$$

The residues are determined by the period conditions

$$A_{\nu,k,i,1}^{\pm} = \pm c_{\nu,k,i},$$

where $c_{\nu,k,i}$ are prescribed real numbers.

As explained in Section 3.1, the coefficients $A_{\nu,k,i,n}$ for $n \geq 2$ may be computed by solving a linear system by iteration. Adapted to the case at hand, this gives the following recipe:

$$A_{\nu,k,i,m+1}^{\pm} \leftarrow -\delta_{m,1}\lambda_{\nu,k} t_{k,i} + (-t_{k,i})^m \sum_{n=1}^{\infty} \binom{n+m-2}{m-1} \times \Bigg[\sum_{\substack{j=1 \\ j\neq i}}^{N_k} \frac{A_{\nu,k,j,n}^{\mp}}{(a_{k,i}^{\mp} - a_{k,j}^{\mp})^{n+m-1}} + \sum_{j=1}^{N_{k\mp1}} \frac{A_{\nu,k\mp1,j,n}^{\pm}}{(a_{k,i}^{\mp} - a_{k\mp1,j}^{\pm})^{n+m-1}} \Bigg]$$

($\delta_{i,j}$ denotes the Kronecker symbol). Namely, we compute the right-hand side for all ν, k, i, and for all $m \geq 1$; we replace all $A_{\nu,k,i,m+1}$ by the values we have found; and we iterate this process until each $A_{\nu,k,i,m+1}$ is equal to the right-hand side to the desired order of accuracy. As was already stated, we also truncate the series to some reasonable order, depending on how small the parameters $t_{k,i}$ are.

The meromorphic 1-forms can be explicitly integrated:

$$\begin{aligned} X_{\nu,k}(z) &= \mathrm{Re}\int \phi_{\nu,k} \\ &= \mathrm{Re}(\lambda_{\nu,k} z) \\ &\quad + \sum_{i=1}^{N_k}\Big(A_{\nu,k,i,1}\log|z-a_{k,i}^-| \\ &\qquad\qquad + \mathrm{Re}\sum_{n=2}^{\infty}\frac{A_{\nu,k,i,n}^-}{(1-n)(z-a_{k,i}^-)^{n-1}}\Big) \\ &\quad + \sum_{i=1}^{N_{k-1}}\Big(A_{\nu,k-1,i,1}\log|z-a_{k-1,i}^+| \\ &\qquad\qquad + \mathrm{Re}\sum_{n=2}^{\infty}\frac{A_{\nu,k-1,i,n}^+}{(1-n)(z-a_{k-1,i}^+)^{n-1}}\Big). \end{aligned}$$

The period problem can be written thus: $X_{\nu,k}(a_{k,i}^- + \sqrt{t_{k,i}}) - X_{\nu,k+1}(a_{k,i}^+ + \sqrt{t_{k,i}})$ is independent of i.

Let $\psi = \phi_1^2+\phi_2^2+\phi_3^2$. Following [Traizet 06], we solve the following equations:

$$\int_{C(a_{k,i}^-,1)}(z-a_{k,i}^-)\frac{\psi}{dz}=0, \qquad (3\text{–}7)$$
$$1\le k\le M,\ 1\le i\le N_k,$$
$$\int_{C(a_{k,i}^+,1)}\frac{\psi}{dz}=0, \qquad (3\text{–}8)$$
$$1\le k\le M,\ 2\le i\le N_k,$$
$$\int_{C(a_{k,i}^-,1)}\frac{\psi}{dz}=0, \qquad (3\text{–}9)$$
$$1\le k\le M,\ 1+2\delta_{k,1}\le i\le N_k,$$
$$\mathrm{Im}\Big(\sum_{i=1}^{2}a_{1,i}^-\int_{C(a_{1,i}^-,1)}\frac{\psi}{dz}\Big)=0. \qquad (3\text{–}10)$$

Provided that the period problem is solved (all periods of ϕ_1, ϕ_2, and ϕ_3 are pure imaginary), ψ also automatically satisfies the following relationship:

$$\sum_{k=1}^{M+1}(-1)^k\left[\sum_{i=1}^{N_k}\int_{C(a_{k,i}^-,1)}z\frac{\psi}{dz}+\sum_{i=1}^{N_{k-1}}\int_{C(a_{k-1,i}^+,1)}z\frac{\psi}{dz}\right] \in i\mathbb{R}. \qquad (3\text{–}11)$$

This mysterious relation is a consequence of Riemann's bilinear relation. For completeness, we give a proof of this relationship in Section 4.4.

By the same argument as in [Traizet 06], one can prove that if t is small enough, these $6N-2M-2$ real equations are linearly independent, so solving this system guarantees that $\psi=0$. For completeness, we provide a proof of this statement in Section 4.5.

Of course, this gives no guarantee that the equations are independent for a given $t>0$, so after solving the equations, we check that ψ indeed vanishes by expanding the series representing it.

4. PROOFS AND COMPUTATIONS

4.1 Dihedral Configurations Are Nondegenerate

In this section we prove that the dihedral configurations of Section 2.2 are nondegenerate for generic values of the parameters $c_1,\dots,c_{M-1}$. As explained in this section, it suffices to find one set of values of the parameters such that the configuration is nondegenerate. We take $a_k = t^{2^k}$ for $1\le k\le M-1$. We shall prove that for $t>0$ small enough, the configuration is nondegenerate.

The idea is the following: Scale the configuration so that the points at level k are the nth roots of unity. Then the points at level $<k$ go to infinity and the points at level $>k$ go to 0 when $t\to 0$, and in the limit we get a Costa–Hoffman–Meeks configuration. So for small t, the configuration may be seen as several overlapping Costa–Hoffman–Meeks configurations. Nondegeneracy thus boils down to the fact that the Costa–Hoffman–Meeks configuration is nondegenerate.

We may normalize $c_1=1$. Then $c_2,\dots,c_{M-1}$ are determined inductively by (2–3), (2–4), and C_M is determined by (2–2). Their limits as $t\to 0$ are

$$\lim c_k = \left(\frac{n-1}{n}\right)^{k-1}$$

for $1\le k\le M-1$ and

$$\lim c_M = \frac{(n-1)^{M-1}}{n^{M-2}}.$$

Tedious computations give the following limits for the partial derivatives of the forces:

$$\begin{aligned} &\lim\Big(t^{2^{k+1}}\frac{\partial F_{k,i}}{\partial p_{k,i}}\Big) \\ &\quad = \lim c_k^2\Big(\frac{n-1}{\omega^{2i}} - 2\sum_{j\ne i}\frac{1}{(\omega^i-\omega^j)^2}\Big), \\ &\lim\Big(t^{2^{k+1}}\frac{\partial F_{k,i}}{\partial p_{k,j}}\Big) = \lim c_k^2\frac{2}{(\omega^i-\omega^j)^2} \quad \text{if } j\ne i, \\ &\lim\Big(t^{2^{k+1}}\frac{\partial F_{k,i}}{\partial p_{k-1,i}}\Big) = 0, \\ &\lim\Big(t^{2^{k+1}}\frac{\partial F_{k,i}}{\partial p_{k+1,i}}\Big) = -\frac{c_k c_{k+1}}{\omega^{2i}}, \end{aligned}$$

$$\lim\left(t^{(4-n)2^{k-1}}\sum_i \omega^i \frac{\partial F_{k,i}}{\partial p_{k,j}}\right) = \lim c_k c_{k-1}\frac{n^2}{\omega^j}$$

with the convention $c_0 = 0$,

$$\lim\left(t^{(4-n)2^{k-1}}\sum_i \omega^i \frac{\partial F_{k,i}}{\partial p_{k-1,j}}\right) = 0,$$

$$\lim\left(t^{(4-n)2^{k-1}}\sum_i \omega^i \frac{\partial F_{k,i}}{\partial p_{k+1,j}}\right) = -\delta_{2,n}\frac{n^2 c_k c_{k+1}}{\omega^j}.$$

Let A be the $n \times n$ complex matrix defined by

$$A_{i,i} = \frac{n-1}{\omega^{2i}} - 2\sum_{j\neq i}\frac{1}{(\omega^i-\omega^j)^2},$$
$$A_{i,j} = \frac{2}{(\omega^i-\omega^j)^2} \quad \text{if } j \neq i.$$

This is the Jacobian matrix of the Costa–Hoffman–Meeks configuration, with the last row and column removed. Since the Costa–Hoffman–Meeks configuration is nondegenerate, A has rank $n-1$, and any minor of size $n-1$ of A is invertible. Let B be the $n \times n$ matrix defined by $B_{i,j} = A_{i,j}$ for $i < n$ and $B_{n,j} = \omega^{-j}$. Then B has rank n. Indeed, the operation $C_n \leftarrow \sum \omega^j C_j$ on the columns of B gives the column $C_n = (0, \dots, 0, n)$.

Returning to the dihedral configuration, put the variables in lexicographic order:

$$p_{1,1},\ \dots,\ p_{1,n},\ \dots,\ p_{M-1,1},\ \dots,\ p_{M-1,n},\ p_{M,1}.$$

From the Jacobian matrix remove the first line, the first column, the last line, and the last column. Let $L_{k,i}$ denote the row corresponding to $F_{k,i}$. Perform the following row operations:

$$L_{k,1} \leftarrow \frac{t^{(4-n)2^{k-1}}}{n^2 c_k c_{k-1}}\sum_i \omega^i L_{k,i} \quad \text{for } k \geq 2,$$
$$L_{k,i} \leftarrow \frac{t^{2^{k+1}}}{c_k^2} L_{k,i} \quad \text{for } k \geq 2,\ i \geq 2.$$

By the above formulas, one obtains a matrix that converges as $t \to 0$ to a matrix that has upper triangular block form, with M square blocks on the diagonal. The first block has size $n-1$ and is an invertible minor of A. The other $M-1$ blocks are equal to B, so are invertible. Hence this limit matrix is invertible. It follows that the dihedral configuration is nondegenerate for t small enough.

4.2 An Asymmetric Configuration of Type 5, 4, 1

In this section we give a proof that there exists a family of embedded asymmetric configurations of type 5, 4, 1. Namely, we take $N_1 = 5$, $N_2 = 4$, $N_3 = 1$. We may normalize $c_1 = 1$, and c_3 is determined as a function of the free parameter c_2 by (2–6). By a straightforward computation, the configuration is embedded, provided that $1 < c_2 < \frac{5-\sqrt{5}}{2} \approx 1.381$.

We first study the case $c_2 = 1$. Equation (2–6) gives $c_3 = 3$. Write

$$P_1 = z^5 + \sum_{i=0}^{4} a_i z^i, \quad P_2 = z^4 + \sum_{i=0}^{3} b_i z^i.$$

We assume that $a_0 \neq 0$, since the case $a_0 = 0$ gives only very symmetric configurations. We also assume that $b_3 \neq 0$, and take $b_3 = 2$ by scaling. Equation (2–5) with $z = 0$ gives $b_1 = 0$. Expanding equation (2–5), we obtain

$$\begin{aligned}&4(1-a_4)z^7 - 6(a_3+a_4-b_2)z^6 - 6(a_2+2a_3)z^5\\ &\quad - 2(2a_1+7a_2-10b_0+2a_3b_2)z^4\\ &\quad - 6(2a_1+a_2b_2-2a_4b_0)z^3 - 6(a_0+a_1b_2-a_3b_0)z^2\\ &\quad - (4a_0b_2-2a_2b_0)z = 0.\end{aligned}$$

Let E_i be the coefficient of z^i in this equation. Write $x = b_2$. Equations $E_7 = 0$ to $E_2 = 0$ in this order determine all coefficients as functions of x by the solution of only linear equations. We obtain, in the given order,

$$\begin{aligned}&a_4 = 1, \quad a_3 = x-1, \quad a_2 = 2-2x,\\ &a_0 = \frac{1}{4}(-4x^3+2x^2+9x-7), \quad a_1 = \frac{1}{4}(6x^2-13x+7),\\ &b_0 = \frac{1}{4}(2x^2-9x+7).\end{aligned}$$

Substituting these values into E_1 gives the equation

$$P(x) := 4x^4 - 4x^3 + 2x^2 - 9x + 7 = 0,$$

which factors as

$$(x-1)(4x^3+2x-7) = 0.$$

This polynomial has four simple roots, two of which are complex. Let x_0 be one of them. Using the Euclidean algorithm, we find that

$$\begin{aligned}D &:= \gcd(P_1, P_2)\\ &= z^3 + (-x_0+2)z^2 + (x_0^2-x_0)z + \frac{1}{4}\left(4x_0^2+2x_0-7\right),\end{aligned}$$

and P_1, P_2 factor as

$$P_1 = (z^2 + (x_0-1)z - x_0 + 1)D, \quad P_2 = (z+x_0)D.$$

In particular, P_1 and P_2 share three roots, so the configuration is singular.

Let us prove that the configuration is asymmetric if x_0 is not real. Let $\varphi : \mathbb{C} \to \mathbb{C}$ be a symmetry of the configuration (other than the identity), so φ fixes the set of roots of P_k, for each $k = 1, 2, 3$. Then $\varphi(0) = 0$, and φ fixes the sum of the roots of P_1, which is equal to 1. Hence $\varphi(z) = \overline{z}$. This implies that the coefficients of P_1 are real, and hence x_0 is real, a contradiction. So the configuration is asymmetric.

For arbitrary values of c_2, we can solve the equations in the same way, except that the computations cannot be explicitly done by hand, so we content ourself with the form of the solutions. In the following, the notation $\ell(\cdot)$ means a linear function of its arguments whose coefficients are rational functions of c_2.

We normalize $b_3 = 1$ and write $b_2 = x$ as before. Then (2–5) has the form

$$\begin{aligned}&\ell(a_4, 1)z^7 + \ell(a_3, a_4, x)z^6 + \ell(a_2, a_3, a_4x)z^5\\ &\quad + \ell(a_1, a_2, a_3x, b_0)z^4 + \ell(a_0, a_1, a_2x, a_4b_0)z^3\\ &\quad + \ell(a_0, a_1x, a_3b_0)z^2 + \ell(a_0x, a_2b_0)z = 0.\end{aligned}$$

Let again E_i be the coefficient of z^i in this equation. Solving the equations $E_7 = 0$, $E_6 = 0$, and $E_5 = 0$ gives $a_4 = p_0(x)$, $a_3 = p_1(x)$, $a_2 = p_1(x)$, where the notation $p_r(x)$ denotes a polynomial of degree at most r in the variable x whose coefficients are rational functions of c_2.

Equations $E_4 = 0$, $E_3 = 0$, and $E_2 = 0$ then give a linear system in the unknowns a_0, a_1, and b_0. The determinant Δ of this system has the form $\Delta = p_1(x)$. Cramer's formula gives

$$a_0 = \frac{p_3(x)}{\Delta}, \quad a_1 = \frac{p_3(x)}{\Delta}, \quad b_0 = \frac{p_3(x)}{\Delta}.$$

Multiplying E_1 by Δ and replacing the above values gives an equation of the form $P(x) = 0$, where P is a polynomial of degree at most 4 whose coefficients are rational functions of c_2.

When $c_2 = 1$, we have seen that that no division by zero occurs in this computation, and P has four simple roots. Therefore, this remains true for generic values of c_2 (that is, except for a finite number of values). Also, for $c_2 = 1$, P has two complex roots. This remains true by continuity for c_2 close to 1.

We have seen in Section 2.3 that for generic values of c_2, the configuration is nonsingular. Let us now prove that it is nondegenerate, provided that it is nonsingular and x_0 is a simple root of P.

Fix the values of c_1, c_2, and c_3. Let $p_{k,i}(t)$ be a deformation of the configuration with $p_{k,i}(0) = p_{k,i}$, where t is a real parameter. Assume that $F_{k,i}(t) = o(t)$. We must prove that up to complex scaling and translation, $p_{k,i}(t) = p_{k,i}(0) + o(t)$.

Normalize translation by $p_{3,1}(t) = 0$, and define as before the polynomials $P_{k,t} = \prod(z - p_{k,i}(t))$. Equation (2–5) gives that

$$\begin{aligned}&c_1^2 z P''_{1,t} P_{2,t} + c_2^2 z P_{1,t} P''_{2,t} - c_1c_2 z P'_{1,t} P'_{2,t} - c_2c_3 P_{1,t} P'_{2,t}\\ &\qquad = o(t)\end{aligned}$$

at the points $p_{1,1}(t), \ldots, p_{1,N_1}(t), p_{2,1}(t), \ldots, p_{2,N_2}(t)$. By linear algebra, the coefficients of the above polynomial are all $o(t)$.

If we call $a_0(t), \ldots, a_4(t)$ and $b_0(t), \ldots, b_3(t)$ the coefficients of $P_{1,t}$ and $P_{2,t}$, normalize scaling by $b_3(t) = 2$, and write $b_2(t) = x_t$, we obtain, by the above computation, the equation $P(x_t) = o(t)$, where P is the same polynomial. (Recall that the coefficients of P depend only on c_2, which is fixed, so P does not depend on t.) Since x_0 is a simple root of P, this implies that $x_t = x_0 + o(t)$. Then we have $a_i(t) = a_i(0) + o(t)$ and $b_i(t) = b_i(0) + o(t)$. Hence $p_{k,i}(t) = p_{k,i}(0) + o(t)$, so the configuration is nondegenerate.

We conclude that if $c_2 > 1$ is close enough to 1, the configuration is nonsingular, nondegenerate, asymmetric, and embedded.

4.3 An Example with a Planar End of Order 2

In this section, we give a computational proof that there exist embedded FTC minimal surfaces with a planar end of order 2. We continue with the example of type 5, 4, 1 of the previous section and take the value $c_2 = \frac{5}{4}$, which gives a planar end at level 2. Here are the results:

$$\begin{aligned}
a_4 &= \frac{5}{24}, \quad a_3 = -\frac{105}{256} + \frac{15}{16}x, \quad a_2 = \frac{3465}{2048} - \frac{4595}{1152}x,\\
a_0 &= -\frac{1}{9437184}\\
&\quad \times \frac{1}{16x+9}\big(-493537968x\\
&\qquad\qquad + 121415679 + 768946176x^3\\
&\qquad\qquad + 162269440x^2\big),\\
a_1 &= \frac{1}{1966080}\\
&\quad \times \frac{1}{16x+9}\big(6967296x^3 - 8351343 + 29794864x\\
&\qquad\qquad - 26814720x^2\big),\\
b_0 &= -\frac{49313}{18432}x + \frac{63}{256}x^2 + \frac{71379}{65536},
\end{aligned}$$

and

$$P(x) = -1524209068800\,x^2 - 285169111920x + 2183134638080x^3 + 180302283315 + 1490178539520x^4.$$

The discriminant of P is

$$137262067070756943236221183727217566386581834266359030391280500736000000,$$

which is nonzero, so P has four simple roots. Each of them gives a nondegenerate configuration.

To prove that each configuration is nonsingular, we use the argument described at the end of Section 2.3. The only values of (m_1, m_2, m_3) that satisfy (2–7), with $m_1 + m_2 \geq 2$ or $m_2 + m_3 \geq 2$, are $(1, 4, 1)$ and $(5, 4, 1)$. Both of them give $P_2 = z^4$, which is not the case because $b_3 = 2$. So the configurations are nonsingular.

Finally, we have

$$c_1 \sum_i p_{1,i} - c_2 \sum_i p_{2,i} = -c_1 a_4 + c_2 b_3 = \frac{55}{24} \neq 0,$$

so the Gauss map has order 2 at the planar end.

4.4 Proof of Equation (3.11)

By the residue theorem, we have

$$\sum_{i=1}^{N_k} \int_{C(a^-_{k,i},1)} z\frac{\psi}{dz} + \sum_{i=1}^{N_{k-1}} \int_{C(a^+_{k-1,i},1)} z\frac{\psi}{dz} = -2\pi \mathrm{i} \mathrm{Res}_{\infty_k}\left(z\frac{\psi}{dz}\right). \tag{4–1}$$

Let g be the genus of Σ and $A_1, \dots, A_g, B_1, \dots, B_g$ a canonical homology basis of Σ. We apply Riemann's bilinear relation [Griffiths and Harris 78, p. 241] to the pair of meromorphic 1-forms (ϕ_1, ϕ_2) (these are meromorphic differentials of the second kind):

$$\sum_{i=1}^{g} \int_{A_i} \phi_1 \int_{B_i} \phi_2 - \int_{A_i} \phi_2 \int_{B_i} \phi_1 = 2\pi \mathrm{i} \sum_{k=1}^{M+1} \mathrm{Res}_{\infty_k}\left(\phi_2 \int \phi_1\right). \tag{4–2}$$

By assumption, the period problem is solved, so all periods of ϕ_1 and ϕ_2 are imaginary. Hence the left side is real.

To compute the residues at ∞_k, we write, in a neighborhood of ∞_k,

$$\phi_1 = dz + \mu_{1,k}\frac{dz}{z^2} + o\left(\frac{dz}{z^2}\right),$$

$$\int \phi_1 = z - \frac{\mu_{1,k}}{z} + o\left(\frac{1}{z}\right),$$

$$\phi_2 = (-1)^{k+1}\mathrm{i}dz + \mu_{2,k}\frac{dz}{z^2} + o\left(\frac{dz}{z^2}\right),$$

$$\phi_3 = Q_k\frac{dz}{z} + o\left(\frac{dz}{z}\right),$$

where $\mu_{1,k}$, $\mu_{2,k}$ are some complex numbers and Q_k is real. This gives

$$\mathrm{Res}_{\infty_k}\left(z\frac{\psi}{dz}\right) = -2\mu_{1,k} + 2(-1)^k\mathrm{i}\mu_{2,k} - Q_k^2,$$

$$\mathrm{Res}_{\infty_k}\left(\phi_2 \int \phi_1\right) = (-1)^{k+1}\mathrm{i}\mu_{1,k} - \mu_{2,k}.$$

Since Q_k is real,

$$\mathrm{Im}\,\mathrm{Res}_{\infty_k}\left(z\frac{\psi}{dz}\right) = 2(-1)^{k+1}\mathrm{Re}\,\mathrm{Res}_{\infty_k}\left(\phi_2 \int \phi_1\right). \tag{4–3}$$

Equations (4–1), (4–2), and (4–3) prove (3–11).

4.5 Proof That the Equations Are Independent

Let ψ be any meromorphic quadratic differential on Σ with at most double poles at $\infty_1, \dots, \infty_{M+1}$. In this section we prove that equations (3–7) to (3–11) imply that $\psi = 0$, provided that t is small enough. The idea is to prove that this is true if $t = 0$, and conclude by continuity.

When $t = 0$, Σ_t is a noded Riemann surface. In this case, the notion of holomorphic quadratic differential must be replaced by that of a regular quadratic differential. A regular quadratic differential ψ is holomorphic outside the nodes (with at most double poles at $\infty_1, \dots, \infty_{M+1}$) and has at most double poles at each side $a^-_{k,i}$ and $a^+_{k,i}$ of each node, with the same residue. (The residue of a q-differential at a pole p is the coefficient of ζ^{-q} in the expansion of ψ in terms of a local coordinate ζ such that $\zeta(p) = 0$. This is independent of the choice of the local coordinate.) The space of regular quadratic differentials on Σ_t depends holomorphically on t, including at $t = 0$.

Let ψ be a regular quadratic differential on Σ_0 satisfying equations (3–7) to (3–11). Since ψ has at most double poles at $\infty_1, \ldots, \infty_{M+1}$, ψ/dz is holomorphic at $\infty_1, \ldots, \infty_k$. Equation (3–7) implies that ψ/dz has at most simple poles at all $a^+_{k,i}$, $a^-_{k,i}$.

Equations (3–8) and (3–9) imply that the only possible poles of ψ/dz are at $a^-_{1,1}$, $a^-_{1,2}$, and $a^+_{k,1}$ for $k = 1, \ldots, M$. Since ψ/dz has at most one simple pole in each $\mathbb{C}_k \cup \{\infty_k\}$, $k \geq 2$, we conclude that $\psi = 0$ in each $\mathbb{C}_k$, $k \geq 2$.

Equations (3–10) and (3–11) imply that

$$a^-_{1,1}\mathrm{Res}_{a^-_{1,1}}\frac{\psi}{dz} + a^-_{1,2}\mathrm{Res}_{a^-_{1,2}}\frac{\psi}{dz} = 0.$$

The residue theorem in $\mathbb{C}_1$ gives

$$\mathrm{Res}_{a^-_{1,1}}\frac{\psi}{dz} + \mathrm{Res}_{a^-_{1,2}}\frac{\psi}{dz} = 0.$$

These two equations imply that ψ/dz has no residue in $\mathbb{C}_1$, so $\psi = 0$.

ACKNOWLEDGMENTS

Maple was used to carry out all numerical computations described in this paper. The domains were triangulated using MATLAB. I would like to thank C. Georgelin for her help in using this package.

REFERENCES

[Costa 84] C. Costa. "Example of a Complete Minimal Immersion in $\mathbb{R}^3$ of Genus One and Three Embedded Ends." *Bull. Soc. Bras. Mat.* 15 (1984), 47–54.

[Costa 89] C. Costa. "Uniqueness of Minimal Surfaces embedded in $\mathbb{R}^3$ with Total Curvature 12π." *J. of Differential Geometry* 30 (1989), 597–618.

[Griffiths and Harris 78] P. Griffiths and J. Harris. *Principles of Algebraic Geometry*. New York: Wiley-Interscience, 1978.

[Hoffman and Meeks 90] D. Hoffman and W. H. Meeks, III. "Embedded Minimal Surfaces of Finite Topology." *Annals of Math.* 131 (1990), 1–34.

[Kapouleas 97] N. Kapouleas. "Complete Embedded Minimal Surfaces of Finite Total Curvature." *J. Differential Geom.* 47 (1997), 95–169.

[Traizet 02] M. Traizet. "An Embedded Minimal Surface with No Symmetries." *J. Differential Geometry* 60 (2002), 103–153

[Traizet 06] M. Traizet. "On the Genus of Triply Periodic Minimal Surfaces." To appear in *Journal of Diff. Geom.*, 2006.

[Weber and Wolf 02] M. Weber and M. Wolf. "Teichmüller Theory and Handle Addition for Minimal Surfaces." *Annals of Math.* 156 (2002), 713–795.

Martin Traizet, Laboratoire de Mathématiques et Physique Théorique, Fédération Denis Poisson, Université de Tours, 37200 Tours, France (martin.traizet@lmpt.univ-tours.fr)

Received July 20, 2007; accepted January 18, 2008.